4-2003

Wide Angle Achromatic Prism Beam Steering for Infrared Countermeasures Applications

Bradley D. Duncan
University of Dayton, bduncan1@udayton.edu

Philip J. Bos
Kent State University - Kent Campus

Vassili Sergan
California State University - Sacramento

Wide-angle achromatic prism beam steering for infrared countermeasure applications

Bradley D. Duncan, MEMBER SPIE
University of Dayton
Electro-Optics Program
300 College Park
Dayton, Ohio 45469-0245
E-mail: brad@udayton.edu

Philip J. Bos, MEMBER SPIE
Kent State University
Liquid Crystal Institute
Materials Science Building
Kent, Ohio 44342

Vassili Sergan
California State University
Department of Physics and Astronomy
6000 J Street
Sacramento, California 95819-6041

Abstract. The design and analysis of achromatic doublet prisms for use in laser beam steering is presented. The geometric relationships describing the maximum steering angle are given, as are discussions of first- and second-order dispersion reduction. Infrared (IR) material alternatives and optimum IR material characteristics for wide-angle achromatic prism beam steering are also investigated. Sixteen materials in 120 different combinations have been examined to date. For midwave IR applications it is shown that the minimum dispersion currently achievable across the full 2 to 5 μm spectrum is 1.7816 mrad at an average maximum steering angle of 45 deg. This is accomplished using LiF/ZnS doublet prisms. Several issues related to the azimuth and elevation angles into which light is steered as a function of prism rotation angles are also presented.
[DOI: 10.1117/1.1556393]

Subject terms: infrared countermeasures; achromatic prism; beam steering; Risley prism; dispersion correction.

Paper 020380 received Sep. 3, 2002; revised manuscript received Sep. 27, 2002; accepted for publication Sep. 27, 2002.

1 Introduction

Protecting military aircraft from infrared (IR) guided missiles is a high priority within the U.S. Air Force. To track a threat, modern IR countermeasure (IRCM) systems are designed to slew a stabilized pointer along the threat's line of sight, as determined by a missile warning system. Traditionally, IRCM beam steering has been achieved using precision two-axis gimbaled mirror pod systems. However, such systems necessarily protrude from the aircraft fuselage, thereby increasing drag. Increased drag reduces endurance, performance, and payload capacity for all airborne platforms, and especially for high-performance fighter aircraft. To address this and other issues, the thrust of the research reported herein centers on the design and optimization of a wide-angle broadband 2 to 5 μm midwave IR (MWIR) laser beam steering apparatus comprised of two rotating achromatic prisms that need not protrude from the aircraft body.

While the concepts of achromatic prism design and prismatic beam steering are themselves not new, their application to MWIR countermeasures present several unique challenges. Typically a discussion of achromatic prisms focuses on thin (i.e., small apex angle) prisms designed to operate over a relatively narrow portion of the visible wavelength (i.e., ~400 to 700 nm) spectrum.[1,2] While novel applications include the use of achromatic prism beam expanders, phase retarders, and planar waveguide couplers, some of which are designed for near-IR applications, most achromatic prisms are designed to be achromatic over at most a 110 nm spectral range.[3–6] In addition, commercially available prism-based laser beam steerers are not typically designed to be achromatic and are generally designed to steer laser beams at most 20 deg off axis.[7,8] By contrast, our requirements dictate that we design a prismatic beam steerer that is capable of steering to at least 45 deg, while remaining achromatic over the entire 2 to 5 μm MWIR spectrum—a challenging spectral range that is 10 times wider than the entire visible spectrum.

This paper first provides a description of the basic concepts of rotating prism beam steering. Next, the geometric relationships describing the maximum steering angle are presented, which, in turn, leads to a discussion of first-order dispersion reduction. The reduction of secondary dispersion is then discussed, after which IR material alternatives and optimum IR material characteristics for wide-angle achromatic prism beam steering are presented. Sixteen different materials in 120 different combinations have been examined to date. It is shown that the minimum secondary dispersion yet achievable is 1.7816 mrad using LiF/ZnS doublet prisms, the properties of which are presented later. Before concluding, the geometry and several issues related to the azimuth and elevation angles into which light is steered as a function of prism rotation angles are also presented.

2 Basic Concepts

The refractive properties of wedge prisms and their ability to deviate and steer light is well known. As can be shown, the deviation angle δ is a function of the incidence angle, the prism's apex angle and the material from which the prism is made.[9] By simply rotating a single prism then, it is possible to steer light along a circular path. Similarly, if light passes through two identical cascaded prisms that are rotated independently, for the case of small deviation angles, light can be steered in any direction falling within a cone-shaped field of regard having a half angle of 2δ, as

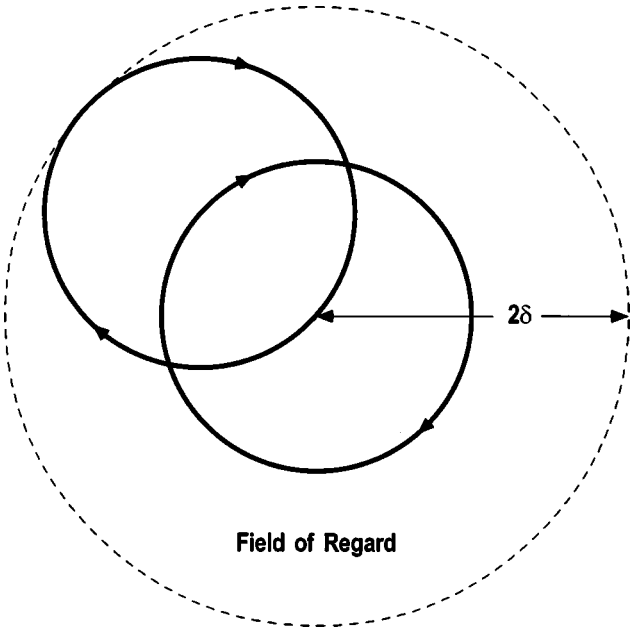

Fig. 1 Ideal beam-steering rosette created using two thin (i.e., small apex angle) coaxial rotating wedge prisms.

shown in Fig. 1.[7,8] (We see in Sec. 7 that the situation becomes rather more complex when large deviation angles are considered.)

Now, simple wedge prisms made of a single optical material can be used effectively to manipulate and steer monochromatic beams of light. However, due to the dispersive nature of optical materials, ''singlet'' prisms cannot be used effectively to steer broadband radiation. In general, as shown in Fig. 2, the shorter ''blue'' wavelengths in a given spectrum are steered to larger angles than are the longer ''red'' wavelengths. On the other hand, as we show, chromatic dispersion in prisms can be nearly fully corrected by

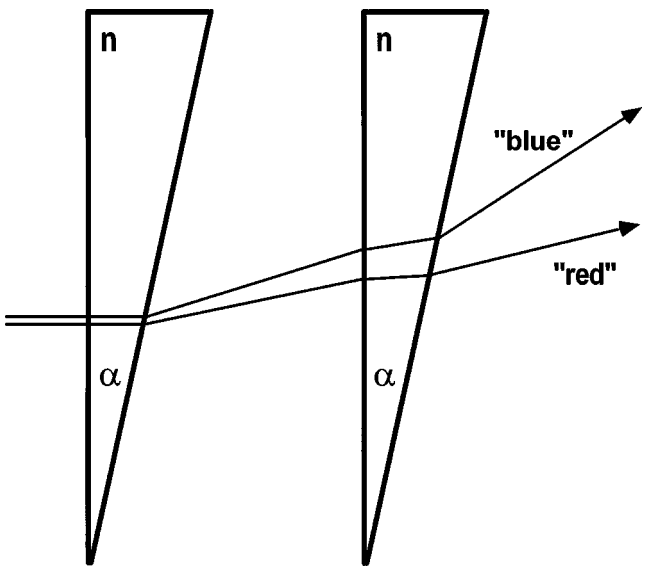

Fig. 2 Singlet prism beam steering is highly dispersive. In general, shorter wavelengths are steered to larger angles than are longer wavelengths.

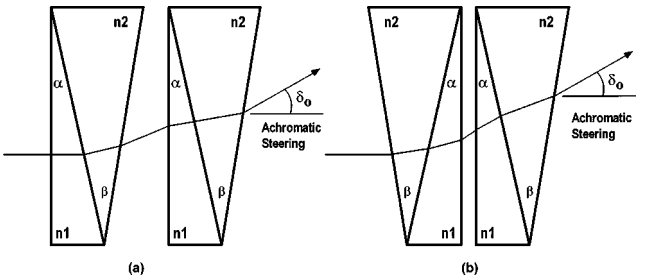

Fig. 3 Alternative achromatic doublet prism beam steering geometries: (a) the forward prism geometry and (b) the reversed prism geometry. While the forward prism geometry provides slightly better dispersion correction, the reversed prism geometry eliminates on-axis blind spots at all wavelengths and is thus preferred.

forming composite ''doublet'' prisms made of two different materials obeying certain properties that are then cemented together. Specifically, we show that with knowledge of the dispersive index characteristics $n(\lambda)$ of appropriate IR materials, the apex angles of two cemented prisms can be chosen to minimize angular dispersion over a broad spectrum, while enabling steering to very wide angles. This, by the way, is exactly the opposite of the design of ''direct view'' or ''direct vision'' prism systems, which are designed for zero angular deviation and maximum angular dispersion.[2]

Two doublet prism geometries are shown in Fig. 3 in their maximum steering angle orientations. In practice, either configuration can be used for the purpose of beam steering. However, though the configuration in Fig. 3(a) may at first seem to be the more natural and/or obvious choice, there are practical advantages to the configuration in Fig. 3(b), which from this point forward is referred to the ''reversed'' prism geometry. The primary advantage of the reversed geometry is that when one prism is rotated by 180 deg with respect to the other, a fully reciprocal optical system is created. This, in turn, means that precise steering to 0 deg is possible at all wavelengths, with no axial blind spot. By contrast, it can be shown that except possibly at discrete wavelengths, the configuration in Fig. 3(a) always has a small but nonnegligible on-axis blind spot—a characteristic that is highly undesirable in any broadband IRCM beam-steering device. For this reason, only the reversed prism geometry is addressed throughout the remainder of this paper. Note, however, that the reversed prism geometry has one disadvantage. By comparing the two configurations in Fig. 3, it is clear that due to the tilted entrance face of the left-hand prism in Fig. 3(b), light passing through the reversed prism geometry suffers dispersive refraction at one additional surface, as compared to the geometry of Fig. 3(a). This, in turn, means that the configuration in Fig. 3(b) will be a bit more dispersive overall than the configuration in Fig. 3(a). In most situations, however, this increase in dispersion is quite small, and the avoidance of an on-axis blind spot by use of the reversed prism geometry far outweighs a modest increase in residual/uncorrected dispersion.

Before presenting the theory relevant to achromatic prism beam steering, we mention one other issue; that is, especially in the field of ophthalmology, the beam-steering devices shown in Figs. 2 and 3 are commonly known as

Risley prisms. When referring to Risley prisms, it is common to discuss the maximum deviation angle in terms of prismatic power Δ, measured in diopters. A single prism diopter is defined to be a deflection of 1 cm at a distance of 1 m from the prism.[7,8] Thus, in general, $\Delta = 100\tan(\delta_0)$, where δ_0 is the maximum deviation of the Risley prism pair, as shown in Fig. 3. For example then, our requirement to steer to at least 45 deg means that we have set out to design a 100-diopter achromatic MWIR Risley prism beam steering device.

3 First-Order Dispersion Reduction

The determination of the maximum steering angle $\delta_0(\lambda)$ for the prism configuration in Fig. 3(b) is found by multiple applications of Snell's law of refraction. Though the process is straightforward, the steps are many. Consequently, only the result is presented here; i.e.,

$$\delta_0(\lambda) = (\alpha-\beta) + \sin^{-1}\left\{ n_2 \sin\left[\beta - \sin^{-1} \times \left(\frac{n_1}{n_2} \sin\left\{ \alpha - \sin^{-1}\left[\frac{\sin\delta_i(\lambda)}{n_1} \right] \right\} \right) \right] \right\}, \quad (1)$$

where α and β are the apex angles indicated in Fig. 3(b), and where the angle $\delta_i(\lambda)$ is the angle at which light exits the first doublet prism and enters the second. This angle is, in turn, given by the following relationship:

$$\delta_i(\lambda) = -\sin^{-1}\left\{ n_1 \sin\left[\alpha - \sin^{-1} \times \left(\frac{n_2}{n_1} \sin\left\{ \beta - \sin^{-1}\left[\frac{\sin(\beta-\alpha)}{n_2} \right] \right\} \right) \right] \right\}. \quad (2)$$

Note that in all cases we have assumed that $n_2 > n_1$ in the prisms shown in Fig. 3(b).

Since the two prisms in Fig. 3(b) are assumed to be identical, we can use the relationship in Eq. (2) to derive a first-order relationship for the reduction of dispersion in our beam-steering apparatus. To begin, we first rewrite Eq. (2) under a small-angle assumption to yield

$$\delta_i(\lambda) \simeq -n_1\left[\alpha - \frac{n_2}{n_1}\left(\beta - \frac{\beta-\alpha}{n_2} \right) \right] = \beta(n_2-1) - \alpha(n_1-1). \quad (3)$$

This approximation is valid for α and β less than $\sim$20 deg—an assumption that we later see is valid in almost all circumstances. Next, we take the derivative of Eq. (3) with respect to wavelength and set the result equal to zero. Solving for β in terms of α, n_1, and n_2 we find

$$\beta = \alpha \frac{n_1'(\lambda_c)}{n_2'(\lambda_c)}, \quad (4)$$

where $n'(\lambda_c)$ indicates the first derivative of the index of refraction, evaluated at wavelength λ_c. Therefore, by choosing apex angles that are related as in Eq. (4) we ensure that dispersion is eliminated in the vicinity of λ_c.

Table 1 LiF and ZnS index of refraction coefficients for use in Eq. (5). Using these coefficients over the 2 to 5 μm MWIR spectrum, the R^2 goodness of fit for both polynomial expansions is greater than 99.98%.

	ZnS	LiF
a_0	2.21672	1.39022
a_1	1.15173×10^{-1}	-2.04593×10^{-3}
a_2	-8.82847×10^{-2}	-1.65179×10^{-3}
a_3	2.96172×10^{-2}	-9.66736×10^{-5}
a_4	-4.67517×10^{-3}	—
a_5	2.81705×10^{-4}	—

Though not required, we typically choose λ_c in the middle of the spectrum of interest; e.g., for the MWIR spectrum we set $\lambda_c = 3.5$ μm.

It is instructive at this point to consider some examples to demonstrate the principles we have just developed. For purposes of these examples we assume that the low-index n_1 material comprising our doublet prisms is LiF, while our high-index n_2 material is ZnS. These are both commonly available materials for use in the IR, and their properties are well known (Janos Technology, Inc., Townsend, Vermont). Using published index data, the indices of refraction $n(\lambda)$ of each of these materials has been modeled according the power series

$$n(\lambda) = \sum_{n=0}^{N} a_n \lambda^n, \quad (5)$$

where the index coefficients a_n are provided in Table 1 under the assumption that the wavelength λ is given in micrometers (Janos Technology, Inc., and Refs. 10 and 11). In addition, the dispersion curves (i.e., index versus wavelength) for LiF and ZnS are shown in Figs. 4 and 5, respectively. From these figures and the polynomial regression formulas, we find that at a central MWIR wavelength of $\lambda_c = 3.5$ μm:

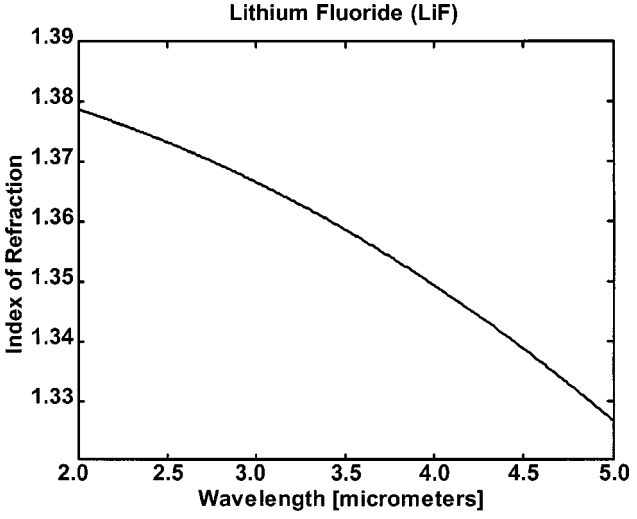

Fig. 4 Dispersive characteristics of LiF over the MWIR spectrum.

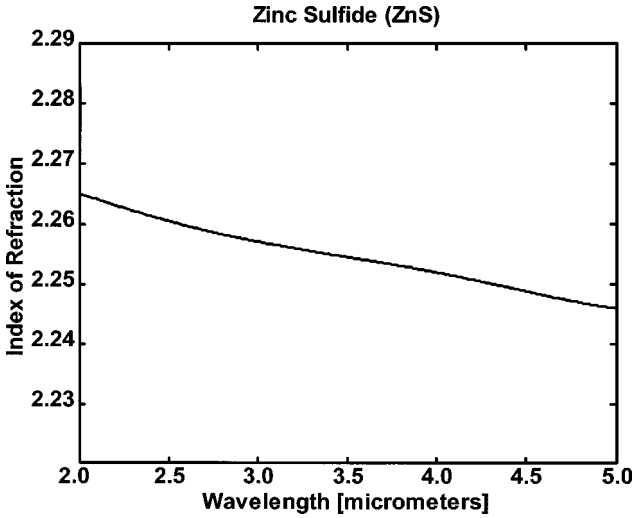

Fig. 5 Dispersive characteristics of ZnS over the MWIR spectrum.

$$n_1 = 1.3587, \quad n_1' = -0.0172/\mu\text{m} \quad (\text{LiF})$$

$$n_2 = 2.2546, \quad n_2' = -0.0048/\mu\text{m} \quad (\text{ZnS}).$$

Then from Eq. (4) we find that, to a first order, dispersion is reduced in the vicinity of 3.5 μm when the apex angle ratio $R = \beta/\alpha = 3.5645$.

Using Eqs. (1) and (2), the dispersive properties of LiF/ZnS doublet prisms configured as shown in Fig. 3(b) are shown in Fig. 6, where the maximum steering angle as a function of wavelength is presented. To generate this figure, the apex angle α was iteratively adjusted to create an average maximum steering angle of 45 deg over the full MWIR spectrum, while β was fixed at 3.5645α. Notice that for LiF/ZnS doublet prisms, the apex angles required for wide-angle steering are quite small, thus lending validity to the small-angle assumptions made in the derivation of Eq. (3).

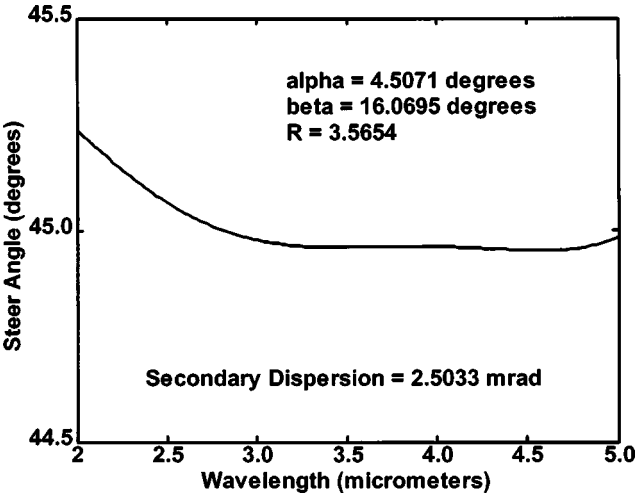

Fig. 6 Steering angle dispersion for LiF/ZnS doublet prisms in the reversed prism geometry. The prism apex angles were adjusted to yield an average maximum steering angle of 45 deg, while for this figure only first-order dispersion reduction at a wavelength of 3.5 μm was addressed.

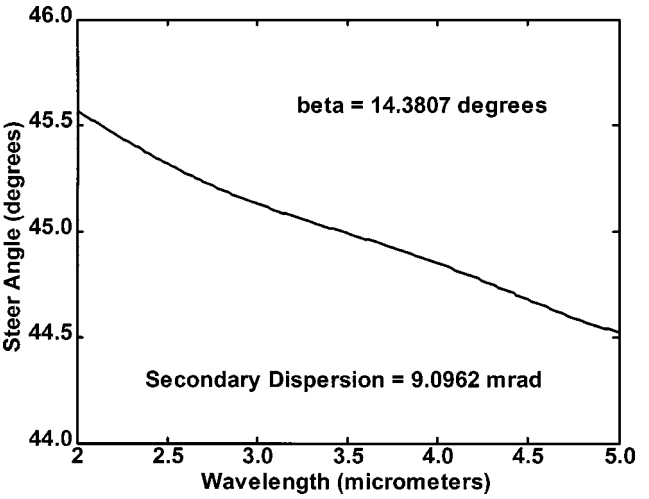

Fig. 7 Steering angle dispersion for ZnS singlet prisms in the reversed prism geometry. The prism apex angles were adjusted to yield an average maximum steering angle of 45 deg.

Notice also that the first-order steering angle dispersion (i.e., slope) in the vicinity of 3.5 μm is precisely zero, as expected, but that the steering angle is clearly still a function of wavelength overall. This residual dependence of steering angle on wavelength is known as secondary dispersion. While a detailed discussion of the reduction of secondary dispersion is reserved to the next section, we define it here to be

$$\Delta\delta_0 = \frac{\delta_0|_{\max} - \delta_0|_{\min}}{2}. \tag{6}$$

For LiF/ZnS prisms, we see from Fig. 6 that under the conditions already stated, the secondary dispersion over the full MWIR spectrum is $\Delta\delta_0 = 2.5033$ mrad, though it is only 0.2897 mrad over the 3- to 5-μm spectral region.

At this point one may wonder whether or not the effort involved in designing achromatic doublet prisms is worth the benefit. Indeed, for beam-steering purposes, do they really perform better than singlet prisms? Figure 7 assists in answering this question. Here the results of using two ZnS-only singlet prisms configured in the reversed prism geometry is shown. To generate this figure, we set n_1 equal to unity and apex angle alpha equal to zero in Eqs. (1) and (2). The apex angle β was then adjusted until the average maximum steering angle was made equal to 45 deg. We see that compared to the results in Fig. 6, secondary steering angle dispersion has increased substantially to $\Delta\delta_0 = 9.0962$ mrad. In addition, by examining Figs. 4 and 5 we see that LiF is more than twice as dispersive as ZnS over the full MWIR spectrum. Although not shown here it is thus clear that steering with two LiF singlet prisms would yield even greater dispersion than two ZnS singlet prisms. We can therefore conclude that the effort required to design achromatic doublet prisms does indeed show great promise in enabling large steering angles to be achieved, while also keeping beam dispersion under tight control.

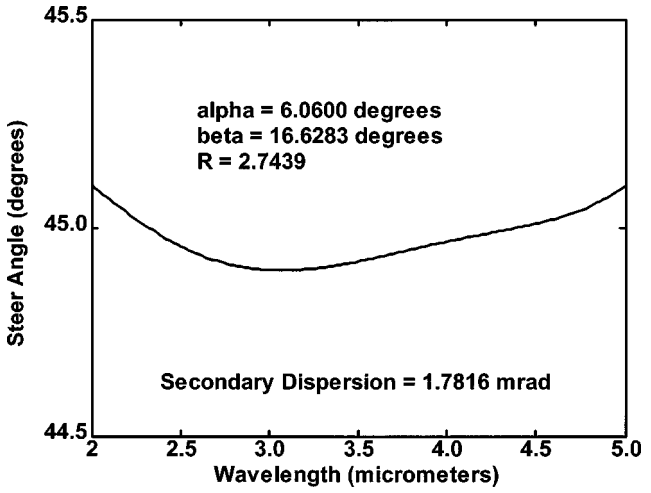

Fig. 8 Steering angle dispersion for LiF/ZnS doublet prisms in the reversed prism geometry. For this figure, the prism apex angles were iteratively adjusted to yield an average maximum steering angle of 45 deg, while also reducing second-order dispersion to a minimum.

4 Reduction of Secondary Dispersion

As we have seen, choosing the apex angle ratio $R=\beta/\alpha$ according to Eq. (4) does cause the steering angle dispersion in the vicinity of λ_c to be exactly zero. However, this choice of R does not necessarily ensure that the more important secondary dispersion is also reduced to a minimum. Unfortunately, there is not a closed form relationship for R, valid for all IR material combinations, that ensures that secondary dispersion is minimized. This is due to the nonlinear dispersive characteristics governing the indices of refraction of the materials, and also the nonlinear behavior of the secondary dispersion $\Delta\delta_0$ as a function of apex angles α and β [see Eqs. (1), (2), and (6)]. As a result, minimization of secondary dispersion is an iterative process generally proceeding according to the following steps:

1. Pick a target value for the average maximum steering angle.
2. Pick starting values for apex angles α and β.
3. Calculate $\delta_0(\lambda)$ according to Eq. (1), and the secondary dispersion according to Eq. (6). Iterate on β until secondary dispersion is minimized.
4. For the current (α,β) combination, calculate the average maximum steering angle.
5. If the average maximum steering angle is different from the target value, increase or decrease α a bit and start again with step 3. [Note from Eqs. (1) to (3) that the steering angles $\delta_0(\lambda)$ generally decrease with increasing α.]
6. When the target average maximum steering angle is achieved, while also having minimized secondary dispersion, determine the optimum apex angles and print/plot the results.

As an example, consider Fig. 8, which was generated using the preceding iterative procedure by assuming LiF/ZnS doublet prisms in the reversed prism geometry. In creating Fig. 8 the apex angles were chosen to minimize secondary dispersion, while also causing an average maximum steering angle of 45 deg. We see that the iterative process results in a decrease in secondary dispersion from 2.5033 mrad in Fig. 6 to only 1.7816 mrad in Fig. 8. This is a reduction of nearly 30%. Notice also in this case that the apex angle ratio has been reduced slightly to $R=2.7439$, while first-order dispersion is now eliminated for wavelengths in the vicinity of 3.1 μm.

5 IR Material Alternatives

For a given average maximum steering angle, the dispersive characteristics of an achromatic doublet prism beam steerer are highly dependant on the materials making up the prisms. Even though IR materials typically exhibit low dispersion, their dispersive nature cannot be ignored when designing achromatic prisms intended for use over a wide spectral range, as is our current task. At this point, it is thus instructive to identify desirable material combination characteristics, and identify alternative combinations of IR materials that can be used.

By careful examination of Eqs. (1) to (3), we can observe that the maximum steering angle δ_0 increases as the ratio n_2/n_1 increases. In addition, δ_0 increases as apex angles α and β decrease and increase, respectively. More specifically, for a given α, δ_0 increases if the apex angle ratio $R=\beta/\alpha$ increases. From Eq. (4), this in turn implies that δ_0 nominally increases as the ratio n_1'/n_2' increases. Regarding the ratio of n_1' to n_2', although it is true that dispersion correction can be performed as long as the slopes of the dispersion characteristics for each of the materials are simply different, it can be shown that it is only when $n_1'>n_2'$ that achromatic steering to large angles can be achieved. Thus, to create achromatic prisms capable of steering to large angles we desire that

$$\frac{n_2}{n_1}>1 \quad \text{and} \quad \frac{n_1'}{n_2'}>1. \tag{7}$$

In fact we prefer these ratios to be as large as possible.

Table 2 provides data for 16 different candidate IR materials (Janos Technology, Inc., and Refs. 10 and 11). Both the nominal indices and the slope of the indices are provided, each of which was calculated at a wavelength of 3.5 μm (i.e., the center of the MWIR spectrum of interest). Based on the data in Table 2, Table 3 shows the minimum achievable secondary dispersion, at an average maximum steering angle of 45 deg, for IR material combinations that satisfy the ratios indicated in Eq. (7). Note that in Table 3 the high-index materials are indicated along the top of the table, while the low-index materials are given in the far left-hand column. All possible combinations of the materials indicated in Table 3 have been investigated thoroughly. The result of this lengthy investigation showed that from among the 32 potentially useful material combinations the best was LiF/ZnS, the optimum steering results for which are shown in Fig. 8. Note that this should not be taken to imply that the LiF/ZnS combination is the universally optimum choice of materials for achromatic prism beam steering. Other materials, as yet not identified or developed, may provide even better results.

Table 2 Index of refraction data for several candidate IR materials.

IR Material	n at 3.5 μm	n' (10^4/m) at 3.5 μm
Ge	4.0308	−2.030
GaAs	3.3081	−0.972
CdTe	2.6884	−0.795
AMTIR-1	2.5144	−0.585
ZnSe	2.4356	−0.490
ZnS	2.2546	−0.481
CsI	1.7439	−0.009
Al_2O_3	1.6953	−3.686
MgO	1.6808	−2.410
IRGN-6	1.5401	−2.360
KBr	1.5362	−0.108
KCl	1.4730	−0.150
BaF_2	1.4591	−0.444
CaF_2	1.4147	−0.830
LiF	1.3587	−1.716
MgF_2	1.3548	−1.109

6 Optimum Material Characteristics

An interesting question now arises. That is, is it possible to specify the refractive index properties of our achromatic prism materials in such a way that dispersion is completely eliminated over the entire 2 to 5 μm spectral range? Interestingly, the answer is yes as we now demonstrate.

From Eq. (4) we see that if we can choose or design materials such that at all wavelengths of interest

$$n_1'(\lambda) = R n_2'(\lambda), \tag{8}$$

where $R = \beta/\alpha$ is a constant, then dispersion can be eliminated completely. Assuming that the high-index material has been specified, using Eq. (5) the index of refraction of the low-index material that satisfies Eq. (8) can be written as

$$\begin{aligned} n_1(\lambda) &= n_1(\lambda_0) + R[n_2(\lambda) - n_2(\lambda_0)] \\ &= n_1(\lambda_0) + R\left[\sum_{n=0}^{N} a_{2n}\lambda^n - \sum_{n=0}^{N} a_{2n}\lambda_0^n\right] \\ &= n_1(\lambda_0) + R\left[\sum_{n=1}^{N} a_{2n}(\lambda^n - \lambda_0^n)\right], \end{aligned} \tag{9}$$

where a_{2n} are the index coefficients of the high-index material, and where λ_0 is a single wavelength at which we must precisely specify the index n_1. For this work we assume $\lambda_0 = 3.5$ μm; i.e., in the middle of the 2 to 5 μm MWIR spectral region.

For purposes of illustration we assume that the high-index material is ZnS, where over the 2 to 5 μm spectral range the index coefficients are provided in Table 1. As we have previously demonstrated, very low dispersion doublet prisms can be created when LiF is paired with ZnS, we also set $n_1(\lambda_0) = n_{\mathrm{LiF}}(3.5\ \mu) = 1.3587$. Furthermore, we will set

$$R = \frac{n'_{\mathrm{LiF}}(3.5\ \ \mu\mathrm{m})}{n'_{\mathrm{ZnS}}(3.5\ \ \mu\mathrm{m})} = 3.5645.$$

By these choices of $n_1(\lambda_0)$ and R we will be able to directly compare LiF to the index profile of the hypothetical material that has been optimized for pairing with ZnS. The index profiles of LiF and the optimized material, which we commonly refer to as BPV-1 (i.e., Brad/Phil/Vassa-1), are shown in Fig. 9. From this figure we see that LiF is very nearly an optimum match to ZnS, in terms of MWIR dispersion correction, over the 3 to 5 μm spectrum, a fact clearly evident from examination of Fig. 6. However, substantial correction is required in the 2 to 3 μm regime. Of course, the greater challenge now is to determine the chemical properties/formulation of BPV-1 so that it can be manufactured. This, however, is left as a topic for further research.

Table 3 Minimum achievable second-order dispersion at an average maximum steering angle of 45 deg. All values are given in milliradians.

		n_2					
		Ge	GaAs	AMTIR-1	ZnSe	CdTe	ZnS
n_1	Al_2O_3	8.833	4.588	3.163	2.057	4.002	1.922
	MgO	9.594	4.735	3.251	2.035	4.118	1.928
	IRGN-6	9.367	4.810	3.368	2.144	4.230	2.084
	MgF_2		4.566	3.102	1.987	3.939	1.835
	LiF		4.380	2.988	1.948	3.770	1.782
	CaF_2			3.292	1.992	4.235	1.869
	BaF_2						
	KCl	No Useful Combinations					
	CsI						
	KBr						

7 Steering Angle Relationships

Now that the techniques by which achromatic prisms can be designed have been presented, it is instructive to examine how the azimuth and elevation angles of a steered beam of light depend on the rotation of the prisms in Fig. 3. [Note that though the arrangement in Fig. 3(b) is preferred for the practical reasons discussed earlier, the following analysis is valid for either prism arrangement in Fig. 3.] Figure 10 depicts the geometry of interest. For small maximum steering angles, when viewed looking into the z axis the bases of the cones in Fig. 10 correspond to the path traced by the ideal steering rosette shown in Fig. 1. In addition, from Fig. 10, we see that if nominal beam propagation is in the z direction, the azimuth angle is measured with respect to the z axis in the y-z plane. The elevation angle is then the angle at which a ray parallel to the exiting beam of light is elevated with respect to the y-z plane.

Now, to address the forward steering problem, refer to Fig. 11. We begin by considering that the exit prism (the right-hand prism in Fig. 3) is held fixed, while the entrance prism is rotated through 2π. The result will be to trace a

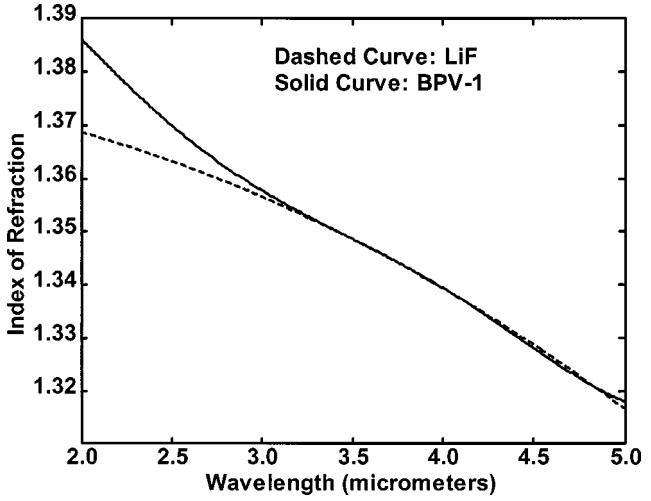

Fig. 9 Comparison of LiF and the hypothetical BPV-1 indices of refraction. We see that LiF is a very good match to ZnS for purposes of dispersion correction over the 3 to 5 μm spectrum, though greater correction is required in the 2 to 3 μm region.

quasi-circular steering path, as shown in Fig. 11(a). [For reference, when the two prisms of Fig. 3 are ''parallel,'' the maximum steering angle is addressed; e.g., $\theta'_{\mathrm{AZ}}=0$, while θ'_{EL} is maximum in Fig. 11(a). Likewise, when the prism's are ''anti-parallel,'' both θ'_{AZ} and θ'_{EL} are zero.] If we then define θ_{1R} to be the rotation of the entrance prism, relative to the exit prism, the effective angle at which light enters the exit prism is given by

$$\delta_i|_{\mathrm{eff}}=\sin^{-1}[\sin(\delta_i)\cos(\theta_{1R})]. \tag{10}$$

In addition, the θ'_{AZ} and θ'_{EL} coordinates of Fig. 11(a) are given by

$$\theta'_{\mathrm{AZ}}=\tan^{-1}[\tan(\delta_i)\sin(\theta_{1R})]$$
$$\theta'_{\mathrm{EL}}=\delta_0|_{\mathrm{eff}}, \tag{11}$$

where θ'_{EL} is found by using Eq. (10) in Eq. (1). We then use Eq. (11) to define the following intermediate variables, which are shown graphically in Fig. 11(a),

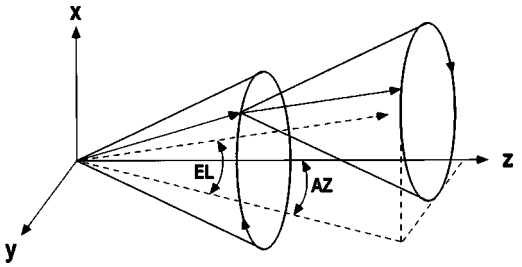

Fig. 10 Azimuth and elevation angle geometry. When viewed looking into the *z* axis, the bases of the cones in this figure correspond to the paths traced by the ideal steering rosette shown in Fig. 1.

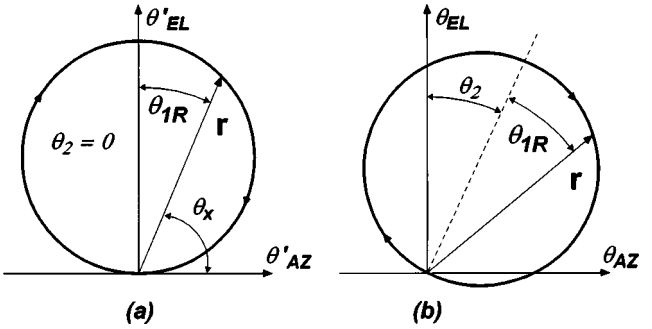

Fig. 11 Steering paths created (a) when the exit prism is held fixed, while the entrance prism is rotated continuously through 2π rad, and (b) when both the entrance and exit prisms are rotated in tandem by an initial angle θ_2, after which the entrance prism is rotated continuously through an additional 2π rad.

$$\theta_x=\tan^{-1}(\theta'_{\mathrm{EL}}/\theta'_{\mathrm{AZ}})$$
$$r=[(\theta'_{\mathrm{EL}})^2+(\theta'_{\mathrm{AZ}})^2]^{1/2}. \tag{12}$$

Now we allow the entrance and exit prisms to rotate in tandem by angle θ_2, as shown in Fig. 11(b). While the exit prism has only been rotated by θ_2, we see that the entrance prism has been rotated by an amount $\theta_1=\theta_{1R}+\theta_2$. As a result, the azimuth and elevation angles ultimately addressed by rotating the entrance and exit prisms by θ_1 and θ_2 are, respectively,

$$\theta_{\mathrm{AZ}}=r\cos(\theta_x-\theta_2),$$
$$\theta_{\mathrm{EL}}=r\sin(\theta_x-\theta_2), \tag{13}$$

where, due to the implicit dependence of Eqs. (13) on the indices of refraction, the azimuth and elevation angles are, strictly speaking, wavelength dependent.

As an example, consider our the lowest dispersion design; i.e., two LiF/ZnS doublet prisms in the reversed geometry, with apex angles $\alpha=6.0600$ deg (LiF) and $\beta=16.6283$ deg (ZnS). Using Eqs. (1), (2), (5), and (10) to (13) we generated the steering angle rosette shown in Fig. 12. In this figure, the inner dashed circle indicates the steering path if only a single LiF/ZnS doublet prism is used, while the large outer dashed circle indicates the maximum steering angle boundary of 45 deg. In addition, the dash-dotted curve shows the small-angle/paraxial steering angle trajectory that would be expected if the exit prism simply doubled the steering angle deflection of the entrance prism. The solid curve, however, shows the actual steering path if the exit prism is held fixed at $\theta_2=0$, while the entrance prism is rotated continuously through 2π rad. Note that the true steering path is only quasi-circular—in fact it is more egg-shaped than truly circular. This very real artifact in the true steering angle path is negligible for very small maximum steering angles; however, as we wish to address maximum steering angles of at least 45 deg, it must be taken into careful consideration.

Next we wish to consider the ''inverse'' steering angle problem. In this case, we wish to first specify the AZ and EL angles to be addressed, and then determine the required

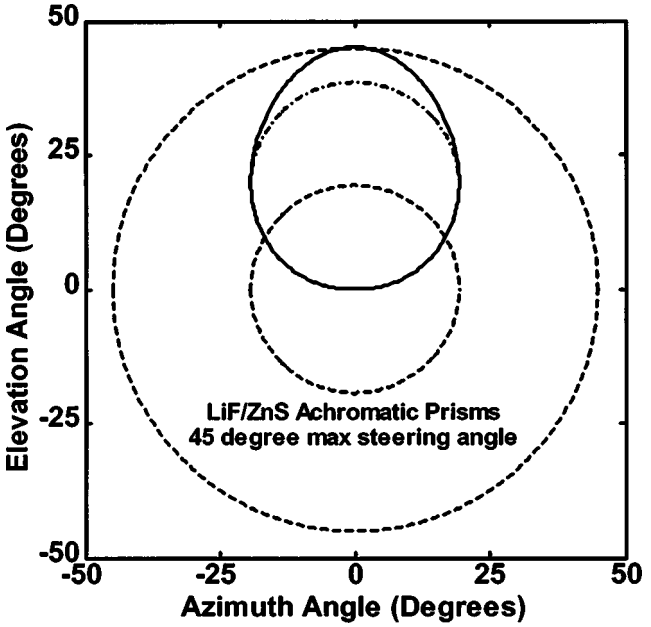

Fig. 12 Actual steering rosette created by use of two LiF/ZnS doublet prisms in their lowest dispersion reversed geometry configuration. The solid curve shows the quasi-circular steering path if the exit prism is held fixed while the entrance prism is rotated through 2π.

rotation of the entrance and exit prisms. By examining Eqs. (1), (2), and (10) to (13), it is clear that this is necessarily a very complex iterative process, though computational speed can be greatly enhanced by the use of look-up tables. Furthermore, it can be shown that for a two-prism beam-steering system, there are exactly two (θ_1, θ_2) solutions for any desired AZ and EL coordinate to be addressed. This simply compounds the complexity of the inverse steering problem solution since we wish to avoid periodic ''flipping'' of one or both of the prisms. In other words, though

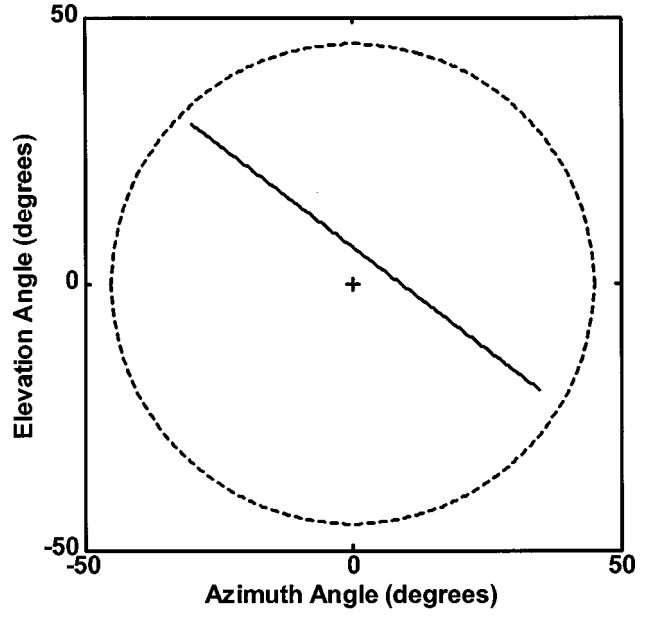

Fig. 13 Example straight-line steering path.

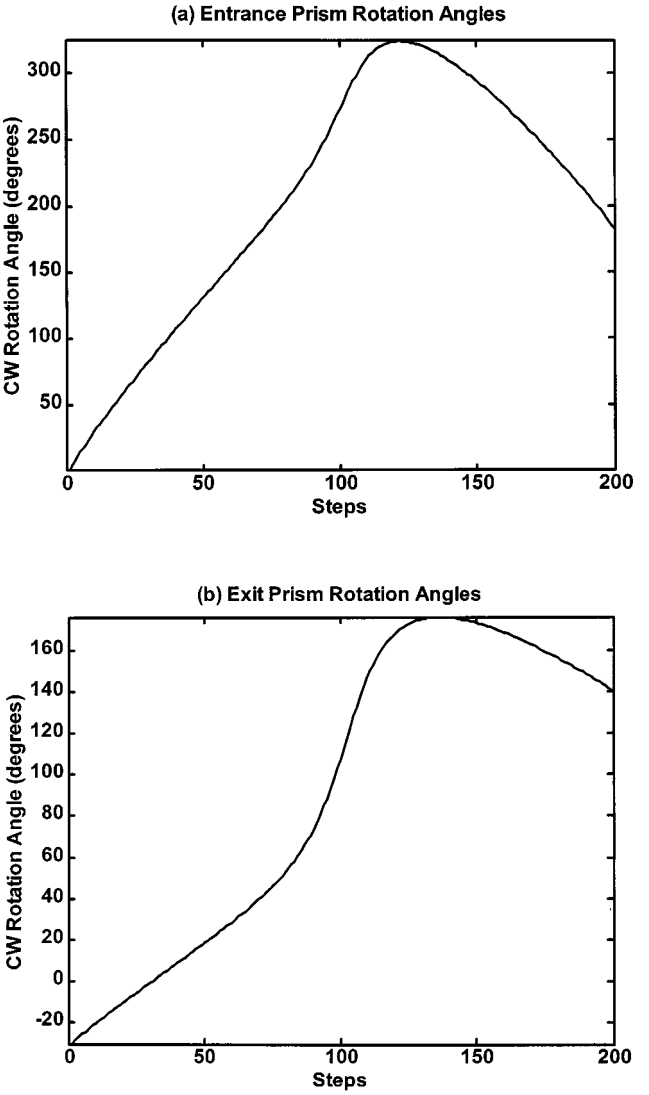

Fig. 14 (a) Entrance and (b) exit prism rotation angles required to steer light along the straight line path shown in Fig. 13. Notice that the rotation angle trajectories are continuous with no discontinuities or singularities.

there are always two (θ_1, θ_2) solutions for any new AZ and EL coordinate to be addressed, we always want to take the shortest angular path and choose the solution that allows for the least amount of change in (θ_1, θ_2) from their current values.

Without discussing the details of the Matlab™ routine used to solve the inverse steering problem, we have been able to demonstrate that for realistic (i.e., smooth) steering paths, the trajectories of θ_1 and θ_2 are strictly continuous, with no singularities, or prism ''flipping'' being required. Two examples are provided here, both of which assume the use of the minimum dispersion LiF/ZnS prisms discussed earlier. In the first example, an arbitrary straight line AZ/EL path was chosen, as shown in Fig. 13. In determining the required entrance and exit prism rotation angle trajectories, we calculated the required θ_1 and θ_2 values as we step through 200 uniformly spaced steps across the desired steering angle path. As shown in Fig. 14, both the entrance and exit prism rotation angle trajectories are strictly con-

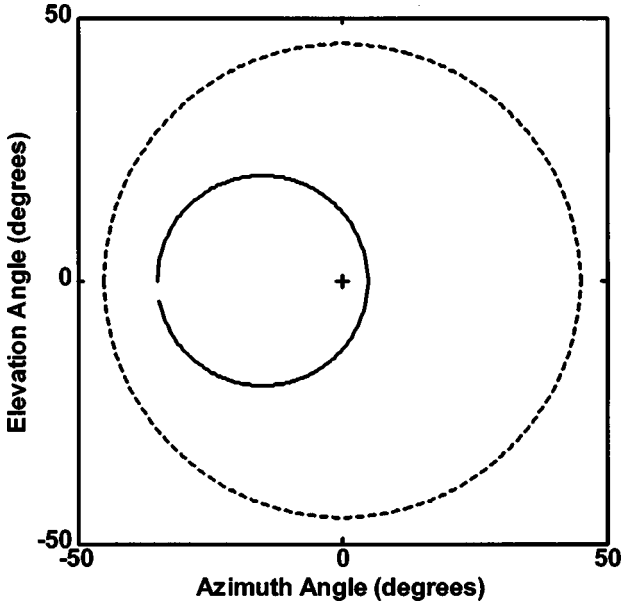

Fig. 15 Example circular steering path.

tinuous, as expected, with no discontinuities or singularities. This is true for all linear paths that were examined, including ones passing through the AZ/EL origin.

In our second example, the circular AZ/EL path shown in Fig. 15 was chosen. Again, in calculating the required entrance and exit prism rotation angle trajectories, we calculated the θ_1 and θ_2 values required as we step through 200 uniformly spaced steps across the desired steering angle path. As shown in Fig. 16, we again see, as expected, that both the entrance and exit prism rotation angle trajectories are strictly continuous, with no discontinuities or singularities.

8 Conclusion

We have seen that the use of two rotating prisms in a Risley beam-steering configuration presents a very promising technology for allowing wide angle steering with very low chromatic dispersion across the wide 2 to 5 μm MWIR spectrum. Though the general concept of using rotating prisms for laser beam steering is not new, there are important issues related to wide-band MWIR beam steering that have never been addressed. These issues include the reduction of secondary dispersion across the entire MWIR spectrum, and the identification of appropriate IR materials to ensure that secondary dispersion is truly minimized in a doublet prism beam-steering arrangement. This paper has presented a summary of our efforts to date in addressing these issues. For example, we have shown in closed form how first-order chromatic dispersion can be reduced by use of doublet prisms. We have also presented the steps that are used to numerically determine optimum apex angles for a doublet prism, for a desired average maximum steering angle, which ensure that secondary dispersion is minimized.

The general characteristics of IR materials appropriate for doublet prism design were also presented, and the results of investigating 16 IR materials in 120 different combinations were provided. To date, the lowest secondary dispersion achieved across the full 2 to 5 μm MWIR spectrum has been 1.7816 mrad for LiF/ZnS doublet prisms in the reversed prism configuration. In addition, the azimuth and elevation angles for a laser beam steered by use of a rotating prism beam-steering device were developed. We have shown that these angles are in general fairly complicated functions of the prism rotation angles, as well as index of refraction and wavelength. However, we have been able to demonstrate that for realistic (i.e., smooth) steering paths, by taking the ''shortest path'' approach, the rotation angle trajectories of the entrance and exit prisms are strictly continuous, with no singularities, or prism ''flipping'' being required.

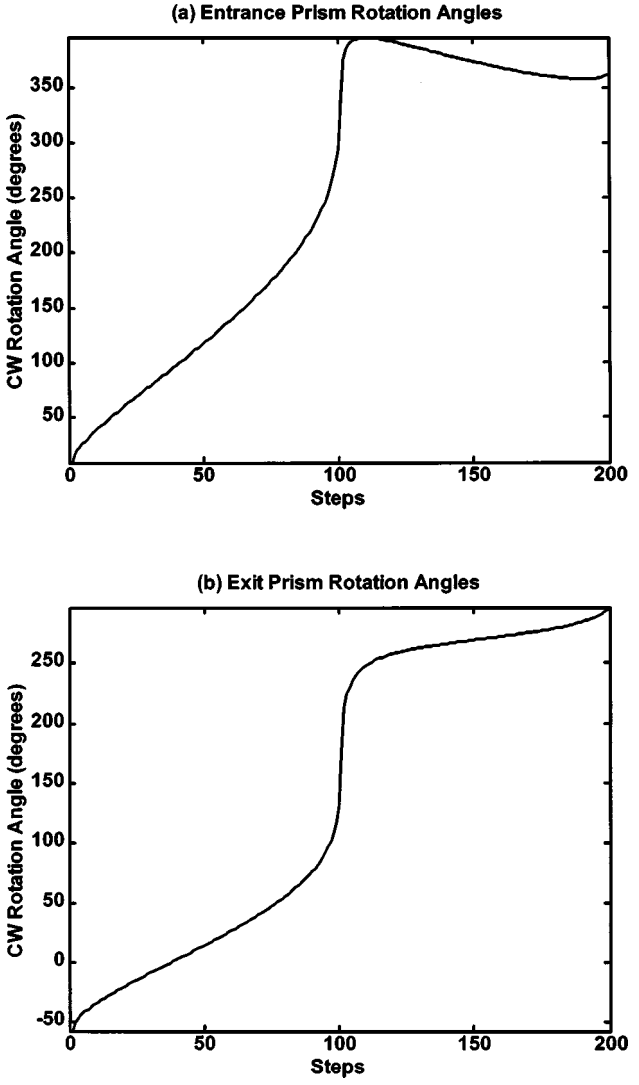

Fig. 16 (a) Entrance and (b) exit prism rotation angles required to steer light along the circular path shown in Fig. 13. As in Fig. 14, the rotation angle trajectories are continuous with no discontinuities or singularities.

Acknowledgments

This research has been supported in part through U.S. Air Force (USAF) Contract No. F33615-00-1-1681. The authors greatly appreciate discussions with Dr. Ed Watson, Dr. Paul McManamon, and Bill Martin of the Air Force

Research Laboratory, Sensors Directorate. We also wish to acknowledge the gracious program support provided by Colonel John Carrano, Defense Advanced Research Projects Agency (DARPA). This paper (USAF Public Affairs Office Document No. ASC 02-1791) has been approved for public release.

References

1. M. Lakin, *Lens Design*, 2nd ed., pp. 259–261, Marcel Dekker, New York (1995).
2. W. J. Smith, *Modern Optical Engineering*, 3rd ed., Chap. 4, McGraw Hill, New York (2000).
3. J. R. M. Barr, ''Achromatic prism beam expanders,'' *Opt. Commun.* **51**(1), 41–46 (1984).
4. H. Fabricius, ''Achromatic prism retarder for use in polarimetric sensors,'' *Appl. Opt.* **30**(4), 426–429 (1991).
5. S. B. Mendes, L. F. Li, J. Burke, and S. S. Saavedra, ''Achromatic prism coupler for planar waveguides,'' *Opt. Commun.* **136**(3–4), 320–326 (1997).
6. K. E. Spaulding and G. M. Morris, ''Achromatic waveguide couplers,'' *J. Lightwave Technol.* **10**(10), 1513–1518 (1992).
7. Edmund Industrial Optics, Inc., *Optics and Optical Instruments Catalog*, Vol. NO21A, p. 64 (2002).
8. Melles Griot, Inc., *The Practical Application of Light*, p. 10.10 (1999).
9. K. D. Möller, *Optics*, Chaps. 1, 7, University Science Books, Mill Valley, CA (1988).
10. Oriel Instruments Inc., *The Book of Photon Tools*, pp. 15-4–15-10, Stratford, CT (2000).
11. GLAD (i.e., General Laser Analysis and Design software), v. 4.6.8, Applied Optics Research, Inc., Austin, TX (2001).

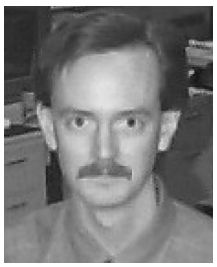

Bradley D. Duncan received his PhD degree in electrical engineering from Virginia Polytechnic Institute and State University (Virginia Tech) in 1991, after which he joined the University of Dayton (UD) faculty. He is now a tenured (full) professor of electrical and computer engineering, with a joint appointment in the graduate electro-optics program. Dr. Duncan's research interests and activities encompass the optical sciences, including the study of ladar systems, photorefractive applications, fiber optic sensor and system technology, integrated optics, nondestructive evaluation, and scanning and nonlinear optical image processing. Dr. Duncan is a member of the OSA, SPIE, and ASEE and a senior member of IEEE. He has been the book reviews editor for *Optical Engineering* and is the faculty advisor for both the University of Dayton student chapter of the OSA, and EΔT, UD's engineering social fraternity. Dr. Duncan directs the research conducted in the UD's National Science Foundation (NSF) Photonics Laboratory, and in 1998 won the Engineering Best Professor of the Year award.

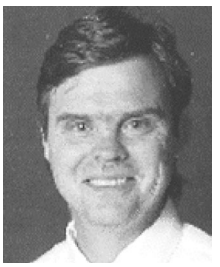

Philip J. Bos received his PhD degree in physics from Kent State University in 1978. After 1 year as a research fellow at Kent State's Liquid Crystal Institute he joined Tektronix Laboratories in the Display Research Department. In 1994 he returned to the Liquid Crystal Institute where he is currently an associate director and a professor of chemical physics. He currently has several projects in the area of applications of liquid crystals. He has over 80 publications and 20 patents.

Vassili Sergan received his PhD degree in physics in 1991 from the Institute of Physics, Ukrainian Academy of Sciences, Kiev, where from 1991 to 1997 he was a researcher. From 1993 to 1995 he was a visiting scientist at the Laboratoir des Phisiques des Solides, Paris University, France, and in 1997 became a research associate with the Liquid Crystal Institute at Kent State University, where he became involved in the Defense Advanced Research Projects Agency (DARPA) steered agile beam (STAB) program. Beginning in the Fall of 2002, he became an associate professor of physics with the California State University at Sacramento. He has produced over 30 publications in the area of liquid crystals.